

Far-IR reflectance spectra analysis of CdZnTe and related materials

Tzuen-Rong Yang^{1,*}, Sheng-Hong Jhang¹, Yen-Hao Shih¹, Fu-Chung Hou², Yu-Chang Yang²,
P. Becla³, Der-Chi Tien⁴ and Zhe Chuan Feng^{2,#},

¹ Department of Physics, National Taiwan Normal University, Taipei, Taiwan 116, ROC

² Graduate Institute of Photonics & Optoelectronics, National Taiwan University, Taipei, Taiwan
106-17, ROC

³ Francis Bitter National Magnet Laboratory, Massachusetts Institute of Technology, Cambridge,
Massachusetts 02139

⁴ Graduate Institute of Mechanical and Electrical Engineering, National Taipei University of Technology,
Taipei 10608, Taiwan, ROC

*corresponding author, Tel: 886-2-29346620-169, Fax: 886-2-22181221, e-mail: yang1@ntnu.edu.tw
e-mail: fengzc@cc.ee.ntu.edu.tw

Abstract

Far-infrared (FIR) reflectance spectroscopy has been employed to study the optical properties for a series of bulk CdZn_xTe_{1-x} and CdSe_xTe_{1-x} wafers. The zone-centre optical phonons for the ternary alloys show a variety of behavior patterns: they exhibit a “one-mode”, “two-mode” or “intermediate-mode” behavior depending on the vibration characteristics of the end binary members. The CdSeTe called CST were found to be single-crystal with the zincblende structure. These four samples labeled with CST5, CST15, CST25, and CST35, which correspond with the composition of Se, 5%, 15%, 25%, 35%, respectively. The intensity of CdTe-like TO band decays with x increasing, and the peak position increases from 140 cm⁻¹ to 145 cm⁻¹. In the other hand, the intensity of CdSe-like TO band grows with x increasing, and the peak position of CdSe-like TO band increases from 174 cm⁻¹ to 181 cm⁻¹. We use the model of dielectric function and using Least-Square fit to find the optical and transport parameters. By the infrared spectra analysis, we found the conductivity of CdZn_xTe_{1-x} increase with increasing of x value and the conductivity of CdSe_xTe_{1-x} decrease with increasing of x value.

I. Introduction

Cadmium telluride, cadmium selenide and their pseudobinary compounds are very suitable for various optoelectronic devices, such as photoconductors, photovoltaic detectors, photo-electro chemical and solar energy cells, and as substrates for growth of quantum wells and epitaxial layers of HgCdTe, HgZnTe and HgMnTe [1, 2]. The II-VI-VI ternary semiconductor CdSe_xTe_{1-x} possesses the zincblende structure for $x < 0.36$. Its energy band gap E_g decreases as x increases in this range. Beyond $x = 0.4$, it exhibits the hexagonal structure with

its energy band gap increasing until it reaches the value for pure CdSe [3]. Several studies of absorption [4] and reflectance [3, 5] reveal that E_g versus Se composition x displays a large bowing effect, with the minimum value of E_g occurring for x between 0.36 and 0.5.

There is considerable variation among data from different authors. Nahory et al. [6] have recently given expressions for the band gaps of the quaternary ZnCdSeTe and its boundary ternary alloys, including CdSe_xTe_{1-x}, as functions of composition at 4 and 300 K. These results

motivate further study of the band gap. Earlier investigations of infrared (IR) reflectance [7,8] and Raman scattering [9] from $\text{CdSe}_x\text{Te}_{1-x}$ have shown the typical two-mode behavior of the long wavelength optical phonons. However, Perkowitz et al. [10] has reported a third mode which was attributed to substantial non-random clustering of the anions around the cations.

We present infrared and theoretical study of five zincblende $\text{CdSe}_x\text{Te}_{1-x}$ crystals with $x = 0$ (i.e. pure CdTe), 0.05, 0.15, 0.25 and 0.35, and confirm that the previously observed third mode seen in infrared spectra is a bulk effect. Using a new type of optical spectrometer, we have successfully obtained room temperature spectra of these alloys, which were not detectable previously using an old type of scanning spectrometer. These data are compared to empirical and to first principles pseudopotential calculations.

The tunable lattice and band properties of $\text{Cd}_{1-x}\text{Zn}_x\text{Te}$ make it a useful Substrate material with potential for devices, and it is an interesting II-VI compound in its own right; yet there has not been much recent optical examination of its unusual phonon modes. In the 1970s, three group-used infrared or Raman spectroscopy to study the transverse-optical (TO) and longitudinal-optical (LO) phonon modes in bulk $\text{Cd}_{1-x}\text{Zn}_x\text{Te}$ at 300K and 80K. All three papers report two-mode behavior,

with similar plots of the CdTe-like and ZnTe-like TO and LO frequencies versus x [11, 12, 13]. All show the remarkable result stated by Vodop'yanov *et al.* [12]; unlike every other two-mode system studied at the time, where one mode's TO frequency increases with x and the other decreases, in $\text{Cd}_{1-x}\text{Zn}_x\text{Te}$ both frequencies grow with x .

II. Experiment

The samples were prepared by the Bridgman technique at Massachusetts Institute of Technology. $\text{CdSe}_x\text{Te}_{1-x}$ alloys were prepared by reacting the 99.9999% pure elemental constituents at $\sim 1150^\circ\text{C}$ in evacuated, sealed quartz tubes. These were regrown by directional solidification at rates of 0.8-1 mm/h in a Bridgman-Stockbarger-type furnace. The resultant boules were cut into slices, 1-2 mm thick, and perpendicular to the growth axis. These were annealed at 650°C in a Se atmosphere, to improve the crystalline perfection. Consequently they were lapped, polished, and etched in a bromine-methanol solution. The alloy compositions were set by the ratio of constituents before growth, and confirmed by X-ray diffraction and transmission measurements after preparation. These samples were found to be single-crystal with the zincblende structure.

The $\text{Cd}_{1-x}\text{Zn}_x\text{Te}$ alloys were made at the Massachusetts Institute of Technology, by

reacting the 99.9999% pure elemental constituents in evacuated and sealed quartz tubes. The sample x values of 0, 0.2, 0.3, 0.5, 0.9 and 1 were calculated from the mass densities. These precast alloys were regrown by directional solidification in a Bridgman-Stockbarger-type crystal-growth furnace. Regrowth occurred at the rate of 1.2mm/h in the furnace adiabatic zone with a temperature gradient of about 15°C/cm. the resulting boules were annealed at 600°C in a Cd-saturated atmosphere for about 5 d. Their surfaces were prepared by lapping, mechanical polish, and etching in bromine-methanol solution.

Fourier transform infrared (FTIR) reflectivity measurements were made using facilities at National Taiwan Normal University described elsewhere [14]. A DTGS detector, for good signal-to-noise ratios-between 40 and 240 cm^{-1} with resolution of 0.1 cm^{-1} were employed to the Bruker IFS66 infrared spectrometer. Data were taken at near-normal incidence and at temperature of 300 K. The incident angle was about 9° degrees, a negligible deviation from normal incidence. The reflection coefficient was measured by ratioing the intensity of the light reflected from the sample against that reflected from a reference mirror made of coin silver with about 99% reflectance.

III. Results and discussion

A. Experiment result

In Figure 1 and Figure 2 display the FTIR reflectivity spectra of the six $\text{CdZn}_x\text{Te}_{1-x}$ sample at 300 and the four $\text{CdSe}_x\text{Te}_{1-x}$ samples, respectively. Below 170 cm^{-1} , the regular reststrahlen band characteristic of the CdTe-like TO phonon is seen in all the samples at 300 K. Beyond 170 cm^{-1} , there is a CdSe-like TO band which grows with x and splits into two bands. From Table 2 we can see that there is a mix mode between CdTe-like TO mode and ZnTe-like TO mode. This indicates that the third peak comes from the bulk, not from the surface, because infrared excitation penetrates into the sample deeply. A bulk origin for the third peak strengthens the earlier interpretation that it comes from non-random cluster effects.

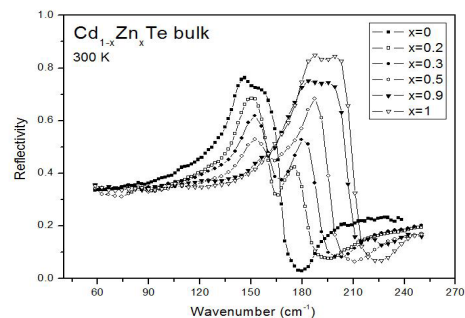


Figure 1. FTIR reflectivity of bulk $\text{Cd}_{1-x}\text{Zn}_x\text{Te}$ at 300 K, with $x = 0, 0.2, 0.3, 0.5, 0.9$ and 1.

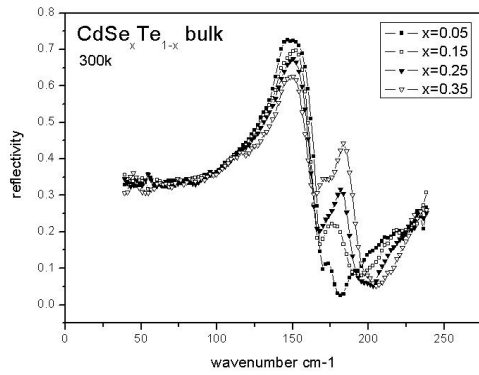


Figure 2. FTIR reflectivity of bulk $\text{CdSe}_x\text{Te}_{1-x}$ at 300 K, with $x = 0.05, 0.15, 0.25,$ and 0.35 .

In Figure 3 and Figure 4 shows the FTIR reflection spectra of $\text{Cd}_{1-x}\text{Zn}_x\text{Te}$ with x from 0 to 1, measured at 300 K, and $\text{CdSe}_x\text{Te}_{1-x}$ with x from 0.05 to 0.35, measured at 300 K. For mixed crystal, there are two x -dependent transverse modes, denoted TO1 and TO2, with oscillator strengths S_1 and S_2 , as shown in Table 1 and Table 2 respectively. Figure 3 shows the FTIR reflection spectra of $\text{Cd}_{1-x}\text{Zn}_x\text{Te}$ with x from 0 to 1, measured at 300 K. The vibration mode occurring in 139.8 cm^{-1} for $x = 0$ at 300 K is referred to as the CdTe-like mode (TO1). Also assign the ZnTe-like mode (TO2) to 180.194 cm^{-1} for $x = 1$ at 300 K. We observed that the CdTe-like TO mode is around $139\text{--}153 \text{ cm}^{-1}$ for different Zn composition at 300 K, and the ZnTe-like TO vibration mode is around $170\text{--}181 \text{ cm}^{-1}$. The vibration mode occurring in 141.3 cm^{-1} in Figure 4 for $x = 0.05$ at 300 K is referred to as the CdTe-like mode (TO1). We can also assign

the CdSe-like mode (TO2) to 174.0 cm^{-1} for $x = 0.05$ at 300 K. We observed that the CdTe-like TO mode is around $141\text{--}146 \text{ cm}^{-1}$ for different Se composition at 300 K, and the CdSe-like TO vibration mode is around $173\text{--}181 \text{ cm}^{-1}$.

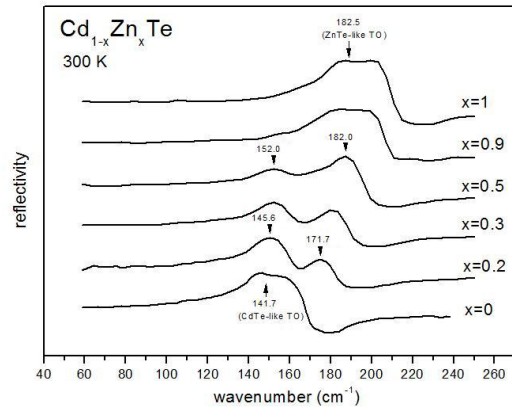


Figure 3. The FIR reflectance spectra of $\text{Cd}_{1-x}\text{Zn}_x\text{Te}$ for Zn composition $x = 0$ to 1 at 300 K.

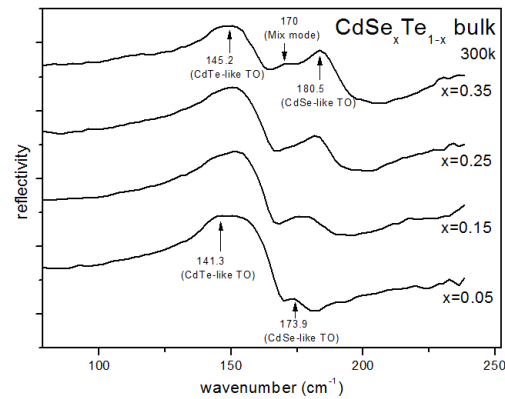


Figure 4. The FIR reflectance spectra of $\text{CdSe}_x\text{Te}_{1-x}$ for Se composition $x = 0.05$ to 0.35 at 300 K.

B. Theoretical fits of FIR reflectance

From a classical model, the FIR dielectric response function can be expressed as

$$\varepsilon(\omega) = \varepsilon_{\infty} + \frac{S_j \omega_{Tj}^2}{(\omega_{Tj}^2 - \omega^2 - i\gamma_j \omega)} - \frac{\omega_p^2}{\omega(\frac{\omega + i}{\tau})}$$

where ε_{∞} is the high frequency dielectric constant, ω_{Tj} , S_j and τ_j are the frequency, strength, and damping constant of the jth TO mode, respectively. The last term in the equation represents the free carrier contribution with a carrier scattering time τ and a plasma frequency

$$\omega_p = \left(\frac{4\pi n e^2}{m^*} \right)^{\frac{1}{2}}$$

where n is the carrier concentration and m^* is the effective mass. Computer Least-Square fittings were performed for all the FIR spectra in Figure 1 and Figure 2. The vibration modes and other parameters of the optical modes at Figure 1 and Figure 2 of 300 K obtained from these theoretical fits are collected in Table 1 and Table 2. The CdTe-like TO, CdSe-like TO vibration modes versus x values are shown in Figure 5 and Figure 6. The values of mode frequency, strength, and phonon relaxation factor or damping constant of each band depend on the detailed composition of samples. The Zn concentration dependence of the strength of CdTe-like and ZnTe-like TO phonon modes is illustrated in Figure 7 and the Se concentration dependence of the strength of CdTe-like and CdSe-like TO phonon modes is illustrated in Figure 8. This shows that the strength of CdTe-like mode is decreasing and the strength of CdSe-like mode

is increasing with increasing Se composition.

From the dielectric function ε for a system with two oscillators, the strength of TO1 and TO2 can be expressed as

$$S_1 \omega_{T1}^2 = \varepsilon_{\infty} \frac{(\omega_{L1}^2 - \omega_{T1}^2)(\omega_{L2}^2 - \omega_{T1}^2)}{\omega_{T2}^2 - \omega_{T1}^2}$$

$$S_2 \omega_{T2}^2 = \varepsilon_{\infty} \frac{(\omega_{L1}^2 - \omega_{T2}^2)(\omega_{L2}^2 - \omega_{T2}^2)}{\omega_{T1}^2 - \omega_{T2}^2}$$

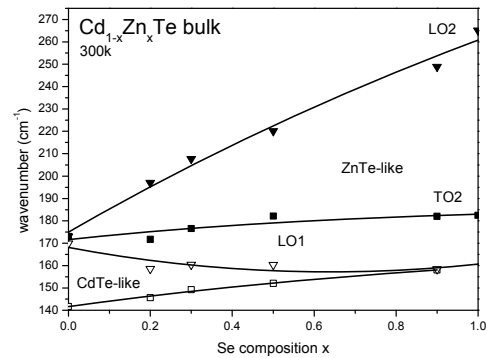


Figure 5. Optical mode frequency versus x from epitaxial $\text{Cd}_{1-x}\text{Zn}_x\text{Te}$ bulk at 300 K. The solid line are the fitting results, and the dash line is the predicted of LO1 and LO2.

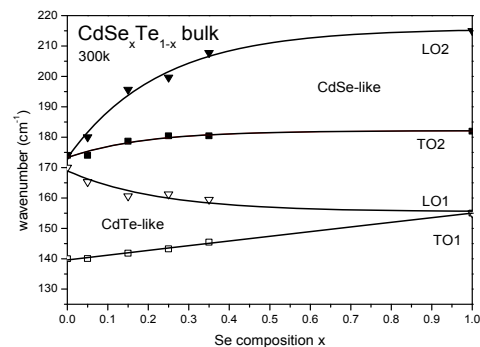


Figure 6. Optical mode frequency versus x from epitaxial $\text{CdSe}_x\text{Te}_{1-x}$ bulk at 300 K. The solid line are the fitting results, and the dash line is the predicted of LO1 and LO2.

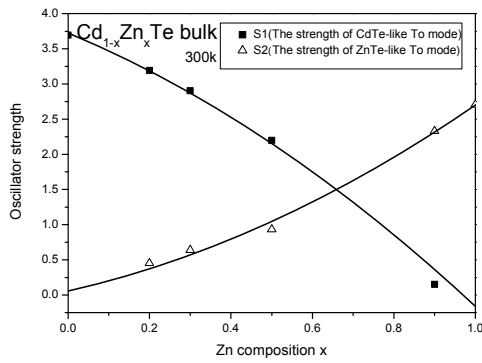


Figure 7. The mode strength of TO1 and TO2 versus Zn composition x at 300 K.

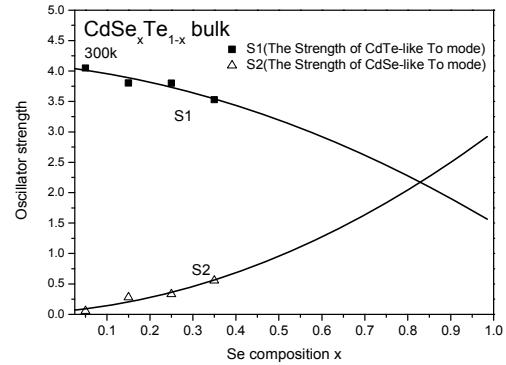


Figure 8. The mode strength of TO1 and TO2 versus Se composition x at 300 K.

C. Electrical conductivity

The electrical properties of these bulk $\text{Cd}_{1-x}\text{Zn}_x\text{Te}$ and $\text{CdSe}_x\text{Te}_{1-x}$ wafers can also be characterized by fitting the dielectric function. The obtained parameter data for the high-frequency limit dielectric constant, free carrier concentration, mobility, conductivity and effective mass are listed in Table 3 and Table 4.

Table 1. Optical constant of $\text{Cd}_{1-x}\text{Zn}_x\text{Te}$ by dielectric function fitting at 300 K.

$\text{Cd}_{1-x}\text{Zn}_x\text{Te}$	300 K	CdTe-like mode			CdSe-like mode		
		ϵ_∞	S_1	$\omega_{\text{TO1}} (\text{cm}^{-1})$	$\gamma (\text{cm}^{-1})$	S_2	$\omega_{\text{TO2}} (\text{cm}^{-1})$
0	8.51546	3.69633	141.742	6.83041			
0.2	8.16634	3.19091	145.638	9.28233	0.45347	171.727	10.858
0.3	7.96	2.90354	149.188	12.9	0.63887	176.518	7.2982
0.5	7.80613	2.19916	152.031	13.7206	0.93155	182.067	5.59974
0.9	7.048	0.15	158	15	2.33075	182	3.98879
1	6.91				3.13523	182.5	3.32447

Table 2. Optical constant of CdSe_xTe_{1-x} by dielectric function fitting at 300 K.

CdSe _x Te _{1-x} 300 K		CdTe-like mode			CdSe-like mode			mix mode		
x	ϵ_{∞}	S ₁	ω_{TO1} (cm ⁻¹)	γ (cm ⁻¹)	S ₂	ω_{TO2} (cm ⁻¹)	γ (cm ⁻¹)	S ₂	ω_{TO2} (cm ⁻¹)	γ (cm ⁻¹)
0.05	8.58989	4.04911	140.064	8.62977	0.05362	173.994	7.53641			
0.15	8.73688	3.80198	141.809	8.0333	0.28025	178.666	17.1627	0.05689	174.476	10.1078
0.25	8.86326	3.93729	142.249	10.4346	0.3339	180.416	11.3184	0.09586	172	10.1078
0.35	9.07434	3.52746	145.459	12.8877	0.55399	180.423	11.8251	0.25081	170	9.7605

Table 3. Electric properties of Cd_{1-x}Zn_xTe characterized by dielectric function fitting at 300 K.

Cd _{1-x} Zn _x Te 300 K Carrier	Concentration	Mobility	Conductivity
x	(10 ¹⁸)	(cm ² /V.s)	m [*] /m _e (ohm-cm ⁻²)
0	2.05741	1.92721	0.11 6.34E-19
0.2	4.82526	1.89733	0.11032 1.46E-18
0.3	4.3513	2.09582	0.11192 1.46E-18
0.5	5.4275	2.78045	0.11798 2.41E-18
0.9	5.49579	6.35942	0.14168 5.59E-18
1	5.39771	7.15874	0.15 6.18E-18

Table 4. Electric properties of CdSe_xTe_{1-x} characterized by dielectric function fitting at 300 K.

CdSe _x Te _{1-x} 300 K Carrier	Concentration	Mobility	Conductivity
x	(10 ¹⁸)	(cm ² /V.s)	m [*] /m _e (ohm-cm ⁻²)
0.05	0.0057	0.91639	0.19655 2.49E-22
0.15	0.00573	0.36328	0.18995 1.59E-22
0.25	0.00567	0.29831	0.18375 2.71E-22
0.35	0.00589	0.23131	0.17795 2.18E-22

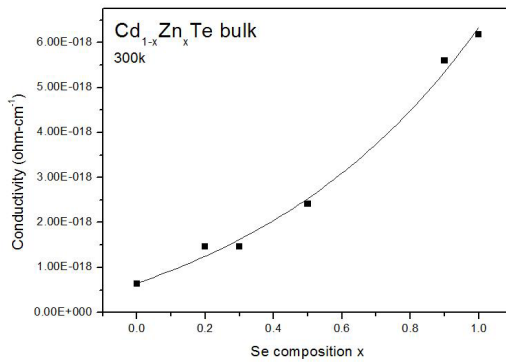


Figure 9. The dependence of the conductivity of the $\text{Cd}_{1-x}\text{Zn}_x\text{Te}$ epilayer with the Zn composition x at 300 K.

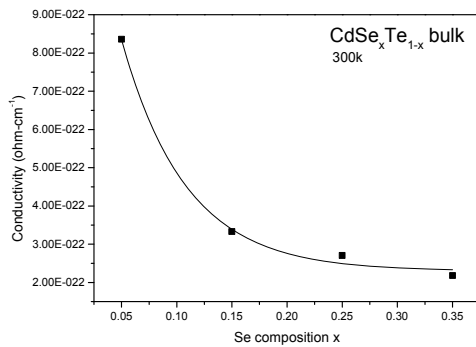


Figure 10. The dependence of the conductivity of the $\text{CdSe}_x\text{Te}_{1-x}$ epilayer with the Se composition x at 300 K.

IV. Conclusion

A multi-technique study using FTIR reflectance has been made on Bridgman-grown bulk $\text{CdSe}_x\text{Te}_{1-x}$ with zincblende structure ($x < 0.36$). We have grown a series of $\text{Cd}_{1-x}\text{Zn}_x\text{Te}$ and $\text{CdSe}_x\text{Te}_{1-x}$ epilayers, with a large range of Zn composition from 0% to 100%, and Se

composition from 15% to 35%. From Figure 9 and Figure 10 we can see that the phonon modes vary by x are regulative, so the far infrared reflection spectra shows the good optical quality of these samples. Theoretical fits through a classical model with the FIR dielectric response function were performed on FIR reflectivity spectra of all the samples. Composition dependent optical parameters of transverse phonon mode frequency, strength, damping constant have been deduced. With an increase of Zn composition x , the CdTe-like TO phonon mode frequency and damping factor increase, but oscillator strength decreases, while the ZnTe-like TO phonon mode frequency and strength increase, and damping factor decreases with increasing x . And with increase of Se composition x , the CdTe-like TO phonon mode frequency and damping factor increase, but oscillator strength decreases, while the CdSe-like TO phonon mode frequency and strength increase, and damping factor decreases with increasing x . Detailed analyses of FIR reflectance and dielectric function have also led to the knowledge of electrical properties of $\text{Cd}_{1-x}\text{Zn}_x\text{Te}$, including the high-frequency limit dielectric constant, free carrier concentration, mobility, conductivity and effective mass. With increasing x , and m^* increase slightly, mobility and conductivity increase greatly. Further analyses of FIR reflectance and

dielectric function have also led to the knowledge of electrical properties of $\text{CdSe}_x\text{Te}_{1-x}$. With increasing x , and m^* increase slightly, mobility and conductivity decrease greatly. These predict a strong effect of Zn and Se composition dependence on the electrical properties of mobility and conductivity, which is useful for device application of this material.

V. References

- [1] S.M. Babu, T. Rajalakshmi, R. Dhanasekaran and P. Bamasamy, *J. Crystal Growth* 110 (1991) 423.
- [2] M. Bouroushian, Z. Loizos, N. Spyrellis and G. Maurin, *Thin Solid Films* 229 (1993) 101.
- [3] M.S. Brodin, N.I. Vitrikhovskii, A.A. Kipen and I.B. Mizetskaya, *Sov. Phys.-Semicond.* 6 (1972) 601.
- [4] L.V. Prytkina, V.V. Volkov, A.N. Mentser, A.V. Vanyukov and P.S. Kireev, *Sov. Phys.-Semicond.* 2 (1968)509.
- [5] H. Tai, S. Nakashima and S. Hori, *Phys. Status Solidi (a)* 30 (1975) K115.
- [6] M.J. Nahory, S.P. Brasel and M. Tamargo, in: *Semiconductor Interfaces and Microstructures*, Ed. Z.C. Feng (World Scientific, Singapore, 1992) p. 238.
- [7] M. Gorska and W. Nazarewicz, *Phys. Status Solidi (b)* 57 (1973) K65; 65 (1974) 193.
- [8] E.A. Vinogradov, L.K. Vodop'yanov and G.S. Oleinik, *Sov. Phys.-Solid State* 15 (1973) 322.
- [9] V.G. Plotnichenko, L.V. Golubev and L.K. Vodop'yanov, *Sov. Phys.-Solid State* 19 (1977) 1582.
- [10] S. Perkowitz, L.S. Kim and P. Becla, *Phys. Rev. B* 43 (1991) 6598.
- [11] H. Narada and S.Narita, *J. Phys. Soc. Jpn.* 30, 1628(1970).
- [12] L. K. Vodop'yanov, E. A. Vinogradov, A. M. Blinov, and V. A. Rukavishnikov, *Fiz. Tverd. Tela (Leningrad)* 14, 268 (1972) [*Sov. Phys.-Solid State* 14,219 (1972)]
- [13] E. A. Vinogradov and L. K. Vodop'yanov, *Fiz. Tverd. Tela (Leningrad)* 17,3161 (1975) [*Sov. Phys.-Solid State*17, 2088 (1976)].
- [14] M. Macler, Z.C. Feng, S. Perkowitz, R. Rousina and J. Webb, *Phys. Rev. B* 46(1992) 6902.